PPPL-2418

J-30169

MICROINSTABILITY-BASED MODELS FOR CONFINEMENT PROPERTIES
AND IGNITION CRITERIA IN TOKAMAKS

By

W.M. Tang, C.M. Bishop, B. Coppi, S.M. Kaye,
F.W. Perkins, M.H. Redi, and G. Rewoldt

FEBRUARY 1987

PLASMA
PHYSICS
LABORATORY PPPL

PRINCETON UNIVERSITY
PRINCETON, NEW JERSEY

MICROINSTABILITY-BASED MODELS FOR CONFINEMENT PROPERTIES

AND IGNITION CRITERIA IN TOKAMAKS

W. M. TANG, C. M. BISHOP[*], B. COPPI[**], S. M. KAYE,

F. W. PERKINS, M. H. REDI, AND G. REWOLDT

Plasma Physics Laboratory, Princeton University

P.O. Box 451, Princeton, New Jersey, USA

ABSTRACT

This paper reports on results of theoretical studies dealing with: (1) the use of microinstability-based thermal transport models to interpret the anomalous confinement properties observed in key tokamak experiments such as TFTR and (2) the likely consequences of the presence of such instabilities for future ignition devices. Transport code simulations using profile-consistent forms of anomalous thermal diffusivities due to drift-type instabilities have yielded good agreement with the confinement times and temperatures observed in TFTR under a large variety of operating conditions including pellet-fuelling in both ohmic-and neutral-beam-heated discharges. With regard to achieving an optimal ignition margin, the adverse temperature scaling of anomalous losses caused by drift modes leads to the conclusion that it is best to operate at the maximum allowable density while holding the temperature close to the minimum value required for ignition.

[*]Permanent Address: Culham Laboratory, UK
[**]Permanent Address: Massachusetts Institute of Technology, Cambridge, MA, USA

MASTER

I. ANALYSIS OF ANOMALOUS THERMAL CONFINEMENT IN TOKAMAKS

Identification of the primary physical processes responsible for the anomalous thermal transport properties currently observed in tokamaks is vitally important not only for the effective development of methods to improve performance in existing devices but also for the proper planning of future ignition experiments. In recent work [1-4] it has been demonstrated that if realistic profile constraints are invoked, then most of the significant confinement trends in low-beta tokamaks can be explained by electrostatic ($\underline{E} \times \underline{B}_o$) transport caused by drift-type microinstabilities. Anomalous thermal transport models based on the associated physics have yielded predictions in very favorable agreement with a substantial experimental data base with respect to both the scaling and the magnitude of the energy confinement time (τ_E) and the central electron temperature (T_{eo}).

In the present studies, the profile-consistent microinstability models derived in Ref. 2 have been used in the BALDUR (time-dependent, 1-D) transport code [5] for the purpose of interpreting experimental results from TFTR including ohmic heating, neutral-beam-injection (NBI) heating, and pellet-fuelling in both ohmic- and NBI-heated discharges. The theoretical expressions for the anomalous thermal diffusivities (χ_e, χ_i) are based on the presence of trapped-electron drift modes and/or toroidal ion temperature gradient (η_i) modes in the bulk region of optimal thermal insulation (roughly located between the $q = 1$ and $q = 2$ surfaces in the plasma). They incorporate the familiar mixing length estimate for the magnitude of the fluctuations and also include the assumption that a temperature "profile consistency" constraint [6] is satisfied. The latter is required here because the present state of development of nonlinear toroidal microinstability theories cannot provide reliable scaling with non-dimensional parameters such as q and because

mechanisms outside the realm of microinstabilities could be playing a prominent role outside the q = 2 region. If the parameter, $\eta_i \equiv d\ln T_i/d\ln n_i$, remains below a critical magnitude, $(\eta_i)_c$ (roughly about 2), then the dominant instability is the trapped-electron mode, and the associated form of the electron diffusivity can be expressed as

$$\chi_e^{TE}(cm^2/sec) = \frac{0.4(1+.25\alpha_n)10^4 P^{0.8} F_H(r)}{n_{eo}R^{1.2}a^{0.1}Z^{0.2}B_T^{0.4}q_a^{0.9}} \qquad (1)$$

with

$$F_H(r) = \frac{[1-\exp(-\alpha_q)]\exp(2\alpha_q r^2/3a^2) \int_0^{r/a} dx x h(x)}{[n_e(r)/n_{eo}] (r^2/a^2)\int_0^1 dx x h(x)} \qquad ,$$

where $\alpha_q = q_a + 0.5$, P(MW) is the total equilibrated ("steady-state") value of the input power (minus radiation losses), h(x) is the energy deposition profile, $n_{eo}(10^{14}~cm^{-3})$, R(m), a(m), $B_T(T)$, and α_n is the usual parabolic density profile parameter. In arriving at Eq. (1), the intrinsic temperature dependence has been eliminated in terms of a power dependence through an assumed thermal steady state [2]. The influence of these modes on χ_i tends to be masked by the usual ion neoclassical transport [2]. However, if $\eta_i > (\eta_i)_c$, then the toroidal η_i-modes become dominant [7], and the associated profile-consistent form of the anomalous ion diffusivity becomes

$$\chi_i^{\eta_i}(r) = \frac{10^3(P/n_{eo})^{0.6}}{(RB_Tq_a)^{0.8}(a)^{0.2}} F_H(r) \qquad . \qquad (2)$$

For a sufficiently collisionless plasma, χ_e also scales as Eq. (2). On the other hand, for values of ν_{*e} (the usual banana regime collisionality parameter) $\gtrsim$ 0.1 to 0.2, the electron loss channel remains sensitive to

collisions in the presence of η_i-modes. This is due to the fact that even though it does not strongly affect these instabilities, the non-adiabatic trapped-electron response does determine χ_e. Hence, the associated form of χ_e tends to be very similar to Eq. (1).

Simulations of nearly two dozen TFTR discharges covering a wide range of experimental conditions were carried out with the BALDUR transport code using $\chi_e = \chi_e^{NEO} + \chi_e^{TE}$, $\chi_i = \chi_i^{NEO} + \chi_i^{\eta_i}$ (with $\chi_i^{\eta_i} = 0$ if $\eta_i \leq 1.5$ at $q = 1.5$). Other important effects such as sawteeth behavior inside the $q = 1$ region, radiation processes, etc. have also been included and are described in Ref. 5. With regard to particle transport, empirical models were constructed to produce density profiles approximating the Thomson-scattering-measured density data. In particular, $D = D^{NEO} + D^{ANOM}$ and $v = v^{NEO} + v^{ANOM}$. For example, in simulating the pellet-fuelled cases, $D^{ANOM}(cm^2/sec) = 4 \times 10^{16}/n_e(r)$ with $v^{ANOM} = 2D^{ANOM}r/a^2$ before and $v^{ANOM} = 0$ after the pellets are injected. The results from the predictive simulations of numerous TFTR large plasma discharges are summarized on Fig. 1 and Table 1. On Fig. 1 the calculated energy confinement times are plotted as a function of the familiar neo-Alcator parameter and compared with the experimental results from a large number of gas-fuelled ohmically heated discharges (crosses) as well as from pellet-fuelled ohmic cases (open diamonds). For the gas-fuelled cases it is quite clear that the anomalous enhancement of χ_i associated with η_i-modes (solid circles) can account for the observed saturation of τ_E at values below those predicted by calculations using only χ_i^{NEO} (open circles). The result from the simulation of an ohmic PDX plasma is also displayed to indicate consistent size-scaling at a small value of the neo-Alcator parameter. With regard to the pellet-fuelled cases the simulation results are again in very good agreement with the experimental data. As shown on Fig. 1, the first pair of

diamonds corresponds to values of τ_E at two points in time after the injection of a single pellet, and the second pair of diamonds to the analogous situation for a three-pellet experiment. The higher τ_E in each pair represents the confinement at the time closer to the time of injection. In these cases the global confinement times are lower than those for the gas-fuelled experiments because of larger energy losses associated with convection and radiation. However, the simulations also indicate that the central confinement is significantly improved after pellet injection because of the resultant peaking in the density profile. This trend, which is in agreement with that found in the TRANSP data analysis, is likely due to χ_e scaling as $1/n_e(r)$ and to the fact that the n_i-driven anomalous enhancement of χ_i can be eliminated (e.g., in the 3-pellet case). Results for τ_E and T_e from simulations of a representative set of NBI-heated TFTR discharges are given in Table 1 and show good agreement with the experimental values. These include a pellet-injection NBI case (shot 14773) and a typical "supershot" discharge (shot 22014). All of the results displayed in Fig. 1 and Table 1 were computed using Eq. (1). With regard to the supershot case, preliminary calculations using a more realistic version of $\chi_e(r)$ (which takes into account only the power into the electron channel and the proper transition into the collisionless regime) has yielded close agreement with the experimental values given in Table 1; i.e., $\tau_E = 0.14$ s and $T_e = 6.2$ keV. In addition, all of the computed temperature profiles correlated well with the data, and comparisons of the theoretical $\chi_e(r)$ given by Eq. (1) and those obtained from TRANSP data analysis studies of a number of ohmic- and NBI-heated TFTR discharges have also indicated reasonable agreement.

Before proceeding with the further development and application of the profile-consistent models just described to the important class of H-mode NBI-

heated divertor plasmas, it is necessary to first establish the proper behavior of the microinstabilities invoked under such conditions. In previous studies involving comprehensive kinetic toroidal computations [8], it was demonstrated that the weaker pressure gradients in the interior region of H-mode plasmas led to correspondingly weaker instabilities. Although this reduction in the local anomalous thermal diffusivity in the inner zone is consistent with the observed improvement in τ_E, it leaves open the question of the nature of the transport properties in the very steep gradient region near the edge. Specifically, in order to be consistent with the thermal fluxes calculated in the interior, the local thermal diffusivity in the edge zone must be greatly reduced. This issue has been addressed in the present work by interfacing the kinetic stability code [8] with a model tokamak equilibrium with a separatrix [9]. The equilibrium here takes into account the enhanced local shear effects near the separatrix and is basically an extension of the familiar "s-α model" [10] whose finite-beta properties are primarily governed by the magnitude of the local pressure gradient. Fully electromagnetic calculations of the dominant toroidal microinstabilities were carried out using as input parameters the edge data obtained from careful measurements of H-mode and L-mode PDX tokamak discharges. The results generally indicate that the proximity of the separatrix to the magnetic surface considered has a significant stabilizing influence. This effect is considerably stronger for the H-mode cases with their characteristically steeper edge profiles. In particular, the finite-beta-modified drift-type electrostatic modes are found to be stable over a region extending several centimeters inside the separatrix for the H-mode profiles but over a much smaller range for the L-mode. These enhanced local stability properties near the separatrix thus serve to support the notion that thermal transport properties in H-mode plasmas are

reconcilable with microinstability-based models.

II. CONSEQUENCES OF MICROINSTABILITIES FOR IGNITION IN TOKAMAKS

The favorable correlations between the confinement trends observed under a large variety of tokamak operating conditions and the results from the anomalous transport studies just described as well as from previous work [1-4] serve to emphasize the importance of addressing the consequences of drift-type instabilities for future ignition devices. Under steady-state conditions, the simplest form of the basic homogeneous (zero-dimensional) thermal energy balance equation is given by

$$P_h = P_{Le} + P_{Li} + P_R - P_\alpha \quad , \tag{3}$$

where P_h is the external heating power density, P_{Le} and P_{Li} represent the losses due to electron and and ion conductivity, P_R represents radiation losses, and P_α is the α-particle heating term. In earlier calculations [11,12] it was demonstrated that the familiar Murakami density limit represents a balance between radiation losses (P_R) and ohmic heating input power (P_h). However, since the fusion power (P_α) will offset P_R at temperatures characteristic of ignition conditions $(T_o > 6$ keV$)$, this limit should not be relevant. Instead, attention needs to be focused on the *influence of enhanced forms of* P_{Le} *and* P_{Li} *caused by the presence of* microinstabilities. First consider the situation where the dominant terms in Eq. (1) are P_α, P_R (from bremsstrahlung), and P_{Le} from anomalous losses associated with the dissipative trapped-electron modes. Using the simple local form for χ_e given in Ref. 1 and applying the boundary conditions of sawtooth flattening for $q \leq 1$ and $T_e = 0$ for $q \geq 2$, the corresponding 1-D

radial equation yields eigenvalue solutions which can be expressed in the form of an ignition criterion,

$$[n_o(10^{15}cm^{-3})B_T(10 \ T)]^2[a(m)]^{2.5}[R(m)]^{1.5} > 14.6(3/q_a)^{1.5}\alpha_n^2 \ . \qquad (4)$$

Since P_{Le} is independent of density in the dissipative trapped-electron regime, it can be concluded that for ignition experiments falling in this regime, the density can be increased to the point where the criterion given by Eq. (4) can be satisfied, provided external power (P_h) is supplied to compensate for the heat capacity of the increased density and to maintain $T_o >$ 6 keV so that $P_\alpha > P_R$. The power required to balance the thermal conduction losses is estimated to be $P_{crit}(MW) = 120 \ (3/q_a)^{2.75} \ (T_o/6 \ keV)^{4.5}$ $\alpha_n^2/(ZB_T^2(aR)^{0.5})$. These results clearly suggest that the optimal ignition scenario would involve operating at (i) the lowest allowable temperature (consistent with ignition), (ii) the highest allowable density (consistent with MHD β-limits but not the Murakami limit), and (iii) the flattest density profiles (because of the strong α_n-dependence in the local model used for χ_e). However, with regard to (iii), it should be strongly cautioned that if the density profiles are allowed to be too flat, then n_i can easily exceed $(n_i)_c$. The consequent enhancement of P_{Li} due to η_i-instabilities can then pose a very restrictive density constraint in the ignition temperature regime. In order to simply illustrate this point, it is convenient to express Eq. (3) in a schematic form highlighting the density and temperature dependences in each term, i.e., (taking $T_i = T_e = T$).

$$P_h - \gamma_{TE} \ T^{9/2} = n^2(\gamma_{BN}T^{1/2} - \gamma_\alpha T^{5/2}) + n\gamma_{\eta_i}T^{5/2} \qquad (5)$$

with $\gamma_{TE}T^{9/2}$ being the dissipative trapped-electron losses, $n^2 T^{1/2}\gamma_{BN}$ being losses due to bremsstrahlung and ion neoclassical conduction, $\gamma_\alpha T^{5/2} \equiv P_\alpha$, and $n\gamma_{n_i}T^{5/2}$ being the n_i-mode losses. In the absence of the last term, Eq. (5) clearly indicates that provided $P_h > \gamma_{TE}T^{9/2}$, there would indeed be no density limit for $T \geq T_{MI}$ with $T_{MI} \equiv (\gamma_{BN}/\gamma_\alpha)^{1/2} \equiv$ minimum ignition temperature. However, if present, this density-dependent loss term would force operating below an upper density bound at $T \leq T_{MI}$ and above a lower density bound at $T > T_{MI}$. The latter situation simply corresponds to requiring $P_\alpha > n\gamma_{n_i}T^{5/2}$. Estimates from Eq. (5) indicate that the external power needed to reach ignition is proportional to $T_{MI}^{9/2}$. Hence, in order to avoid such stringent constraints, pellet-injection-fuelling procedures could be adopted to produce density profiles sufficiently peaked to suppress the n_i-modes. After exceeding the required ignition temperature, a less discriminating fuelling system would be adequate since P_α could then offset any ensuing anomalous losses of this type. In general, for $T > T_{mI}$, the power losses resulting from drift modes increase at least as rapidly with T as the fusion power. Consequently, the optimum path to ignition should exploit favorable scalings with B_T, density, size, etc., while holding T close to T_{mI}.

ACKNOWLEDGMENTS

We are indebted to P.C. Efthimion, G.L. Schmidt, D.R. Mikkelsen, and the TFTR physicists for providing the data as well as valuable assistance needed to carry out the BALDUR simulations. Special thanks are extended to S. Hiroe, P. LeBlanc, and B. Grek for providing the profile data from PDX used in the H-mode calculations.

REFERENCES

[1] PERKINS, F.W., Proc. 4th Int. Symp. on Heating in Toroidal Plasmas, Rome, 1984, Vol. 2, p. 977; PERKINS, F.W., SUN, Y.C., Princeton Plasma Physics Laboratory Report No. PPPL-2261 (1985).

[2] TANG, W.M., Princeton Plasma Physics Laboratory Report No. PPPL-2311 (1986), Nucl. Fusion (in press).

[3] DOMINGUEZ, R.R., WALTZ, R.E., GA Technologies Rep. GA-18184 (1986).

[4] ROMANELLI, F., TANG, W.M., WHITE, R.B., Princeton Plasma Physics Laboratory Report No. PPPL-2310 (1986), Nucl. Fusion (in press).

[5] SINGER, C.E., et al., Princeton Plasma Physics Laboratory Report No. PPPL-2073 (1986).

[6] COPPI, B., Comments Plasma Phys. Cont. Fusion $\underline{5}$, 261 (1980).

[7] TANG, W.M., REWOLDT, G., CHEN, L., Princeton Plasma Physics Laboratory Report No. PPPL-2337 (1986), Phys. Fluids (in press).

[8] TANG, W.M., et al., Nucl. Fusion $\underline{25}$, 151 (1985); REWOLDT, G., et al., Phys. Fluids $\underline{25}$, 480 (1982).

[9] BISHOP, C.M., Culham Laboratory Rep. CLM-P764 (1985).

[10] CONNOR, J.W., et al., Phys. Rev. Lett. $\underline{40}$, 396 (1978).

[11] PERKINS, F. W., HULSE, R. A., Phys. Fluids $\underline{28}$, 1837 (1985).

[12] COPPI, B., TANG, W. M., Princeton Plasma Physics Laboratory Report No. PPPL-2343 (1986).

Table 1. Parameters of Simulated Neutral-Beam-

Heated TFTR Shots

marker: -12-

Shot	$I_p^{(MA)}$	$B_Z^{(T)}$	$R^{(m)}$	$A^{(m)}$	$\bar{n}_e(10^{19}m^3)$	$P_{inj}(MW)$	Z_{eff}	q_a	$T_e^{exp}(keV)$	T_e^{Sim}	$\tau_E^{exp}(s)$	τ_E^{Sim}	$\nu_{*e}^{(q=1.5)}$
14727	2.2	4.8	2.56	0.82	4.8	5.3	2.6	2.8	4.0	3.6	0.20	0.18	0.19
14773	2.2	4.7	2.57	0.82	3.0(7.0*)	5.7	1.9	2.8	2.4	2.8	0.14	0.19	0.29
19965	2.2	4.8	2.49	0.83	4.2	8.8	3.2	3.0	3.8	3.7	0.11	0.11	0.25
22014	0.8	4.6	2.55	0.82	3.2	11.3	2.5	7.6	5.8	3.5	0.12	0.06	0.13
										6.2†		0.14†	

*After Pellet Injection

†Collisional Model
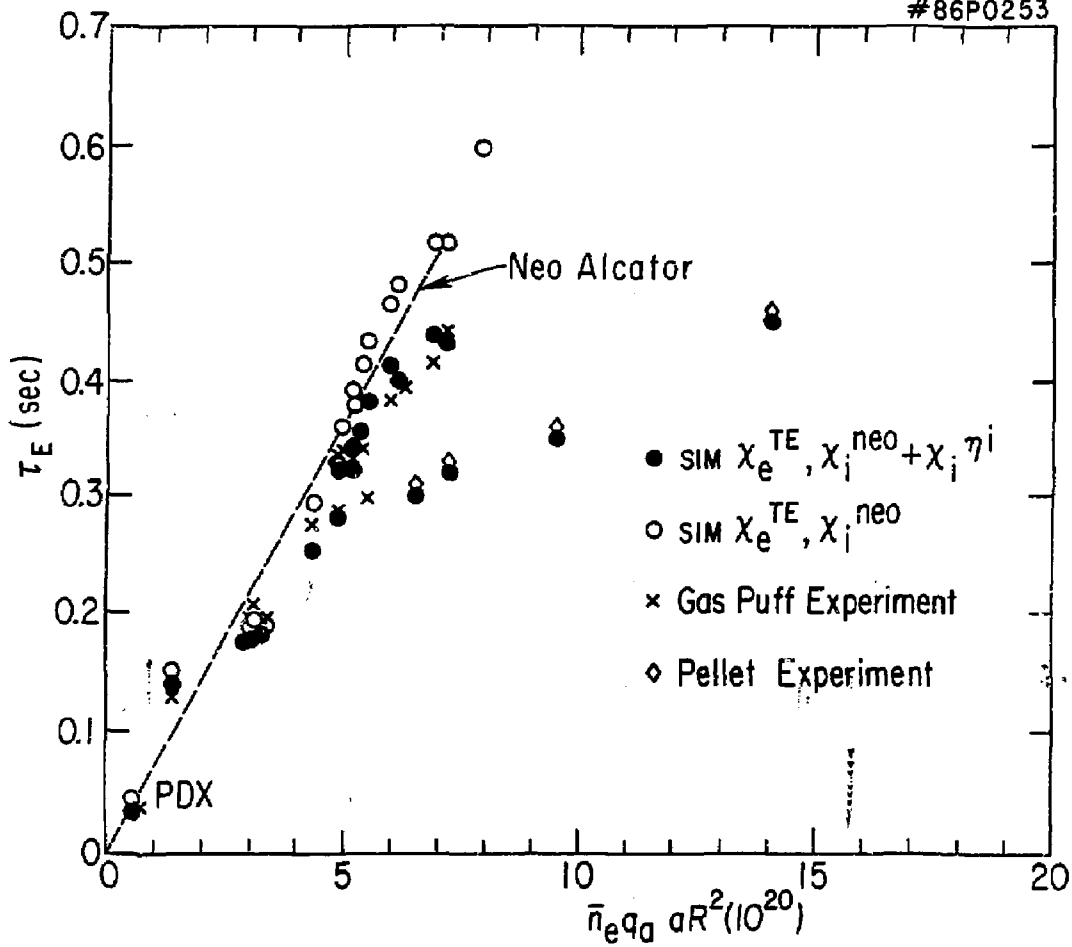
Fig. 1

Dr. Frank J. Paoloni, Univ of Wollongong, AUSTRALIA
Prof. M.H. Brennan, Univ Sydney, AUSTRALIA
Plasma Research Lab., Australian Nat. Univ., AUSTRALIA
Prof. I.R. Jones, Flinders Univ., AUSTRALIA
Prof. F. Cap, Inst Theo Phys, AUSTRIA
Prof. M. Heindler,Institut fur Theoretische Physik,AUSTRIA
M. Goossens, Astronomisch Instituut, BELGIUM
Ecole Royale Militaire, Lab de Phys Plasmas, BELGIUM
Com. of European, Dg XII Fusion Prog, BELGIUM
Prof. R. Boucique, Laboratorium voor Natuurkunde, BELGIUM
Dr. P.H. Sakanaka, Univ Estadual, BRAZIL
Instituto De Pesquisas Espaciasi-INPE, BRAZIL
Library, Atomic Energy of Canada Limited, CANADA
Dr. M.P. Bachynski, MPB Technologies, Inc., CANADA
Dr. H.M. Skarsgard, Univ of Saskatchewan, CANADA
Dr. H. Barnard, University of British Columbia, CANADA
Prof. J. Teichmann, Univ. of Montreal, CANADA
Prof. S.R. Sreenivasan, University of Calgary, CANADA
Prof. Tudor W. Johnston, INRS-Energie, CANADA
Dr. C.R. James, Univ. of Alberta, CANADA
Dr. Peter Lukac, Komenskeho Univ, CZECHOSLOVAKIA
The Librarian, Culham Laboratory, ENGLAND
Mrs. S.A. Hutchinson, JET Library, ENGLAND
C. Mouttet, Lab. de Physique des Milieux Ionises, FRANCE
J. Radet, CEN/CADARACHE - Bat 506, FRANCE
Dr. Tom Musi, Academy Bibliographic, HONG KONG
Preprint Library, Cent Res Inst Phys, HUNGARY
Dr. B. Dasgupta, Saha Inst, INDIA
Dr. R.K. Chhajlani, Vikram Univ. INDIA
Dr. P. Kaw, Institute for Plasma Research, INDIA
Dr. Phillip Rosenau, Israel Inst Tech, ISRAEL
Prof. S. Cuperman, Tel Aviv University, ISRAEL
Librarian, Int'l Ctr Theo Phys, ITALY
Prof. G. Rostagni, Univ DI Padova, ITALY
Miss Clelia De Palo, Assoc EURATOM-ENEA, ITALY
Biblioteca, del CNR EURATOM, ITALY
Dr. H. Yamato, Toshiba Res & Dev, JAPAN
Prof. I. Kawakami, Atomic Energy Res. Institute, JAPAN
Prof. Kyoji Nishikawa, Univ of Hiroshima, JAPAN
Direc. Dept. Lg. Tokamak Res. JAERI, JAPAN
Prof. Satoshi Itoh, Kyushu University, JAPAN
Research Info Center, Nagoya University, JAPAN
Prof. S. Tanaka, Kyoto University, JAPAN
Library, Kyoto University, JAPAN
Prof. Nobuyuki Inoue, University of Tokyo, JAPAN
S. Mori, JAERI, JAPAN
M.H. Kim, Korea Advanced Energy Research Institute, KOREA
Prof. D.I. Choi, Adv. Inst Sci & Tech, KOREA
Prof. B.S. Liley, University of Waikato, NEW ZEALAND
Institute of Plasma Physics, PEOPLE'S REPUBLIC OF CHINA
Librarian, Institute of Phys., PEOPLE'S REPUBLIC OF CHINA
Library, Tsing Hua University, PEOPLE'S REPUBLIC OF CHINA

Z. Li, Southwest Inst. Physics, PEOPLE'S REPUBLIC OF CHINA
Prof. J.A.C. Cabral, Inst Superior Tecn, PORTUGAL
Dr. Octavian Petrus, AL I CUZA University, ROMANIA
Dr. Johan de Villiers, Plasma Physics, AEC, SO AFRICA
Prof. M.A. Hellberg, University of Natal, SO AFRICA
Fusion Div. Library, JEN, SPAIN
Dr. Lennart Stenflo, University of UMEA, SWEDEN
Library, Royal Inst Tech, SWEDEN
Prof. Hans Wilhelmson, Chalmers Univ Tech, SWEDEN
Centre Phys des Plasmas, Ecole Polytech Fed, SWITZERLAND
Bibliotheek, Fom-Inst Voor Plasma-Fysica, THE NETHERLANDS
Dr. D.D. Ryutov, Siberian Acad Sci, USSR
Dr. G.A. Eliseev, Kurchatov Institute, USSR
Dr. V.A. Glukhikh, Inst Electro-Physical, USSR
Dr. V.T. Tolok, Inst. Phys. Tech. USSR
Dr. L.M. Kovrizhnykh, Institute Gen. Physics, USSR
Prof. T.J.M. Boyd, Univ College N Wales, WALES
Nuclear Res. Establishment, Julich Ltd., W. GERMANY
Bibliothek, Inst. Fur Plasmaforschung, W. GERMANY
Dr. K. Schindler, Ruhr Universitat, W. GERMANY
ASDEX Reading Rm, IPP/Max-Planck-Institut fur
   Plasmaphysik, W. GERMANY
Librarian, Max-Planck Institut, W. GERMANY
Prof. R.K. Janev, Inst Phys, YUGOSLAVIA